

# MnSb<sub>2</sub>O<sub>6</sub>-chitosan nanocomposite: An efficient catalyst for the synthesis of coumarins via Pechmann reaction

Baharak Bahramnezhad | Dadkhoda Ghazanfari | Enayatollah Sheikhsosseini |  
Mohammad Reza Akhgar | Sayed Ali Ahmadi

Department of Chemistry, Kerman Branch, Islamic Azad University, Kerman, Iran

## Correspondence

Dadkhoda Ghazanfari, Department of Chemistry, Kerman Branch, Islamic Azad University, Kerman, Iran.  
Email: ghazanfari@iauk.ac.ir

## Abstract

In this work, MnSb<sub>2</sub>O<sub>6</sub>-chitosan nanocomposites were synthesized and have been employed in Pechmann condensation for the synthesis of coumarin derivatives. MnSb<sub>2</sub>O<sub>6</sub>-chitosan nanocomposites were characterized by Fourier transform infrared (FTIR), X-ray powder diffraction (XRD), scanning electron microscope (SEM), and energy-dispersive X-ray spectroscopy (EDX) techniques. The particles of MnSb<sub>2</sub>O<sub>6</sub>-chitosan have uniform spheres with sizes that are less than 100 nm. Simplicity, easy work-up, and short reaction times are advantages of this reaction. Also, we evaluated the antibacterial activity for some of the products, and the result showed significant pharmaceutical activities as antibacterial reagents against *Staphylococcus aureus* and *Escherichia coli*.

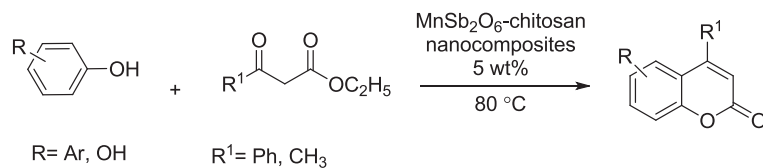
## 1 | INTRODUCTION

Coumarin and its derivatives are an important building block in a variety of natural products and are an important group of heterocyclic compounds, which has attracted considerable attention from organic and medicinal chemists due to its application in the synthesis of organic compounds and biologically active compounds.<sup>[1]</sup> Coumarin and its derivatives have found applications as anticoagulants,<sup>[2]</sup> as additives in food and cosmetics,<sup>[3]</sup> and in the synthesis of insecticides.<sup>[4]</sup> They have also found application in fluorescent probes due to their high chromogenic and fluorogenic properties.<sup>[5]</sup>

Therefore, the design of a new and effective method for the preparation of coumarin and its derivatives should be obtained. Pechmann,<sup>[6]</sup> Perkin,<sup>[7]</sup> Knoevenagel,<sup>[8]</sup> Reformatsky,<sup>[9]</sup> and Wittig reaction<sup>[10]</sup> in the presence of both acidic and basic catalysts<sup>[11,12]</sup> are several suitable methodologies for the synthesis of coumarin and its derivatives. The most widely used method for the preparation of coumarins is Pechmann

reaction. The process consists of the condensation of phenol derivatives with  $\beta$ -keto ester derivatives giving the coumarin derivatives. Different catalysts have been used in Pechmann reaction: Nafion,<sup>[13–15]</sup> amberlyst,<sup>[15,16]</sup> montmorillonite clay,<sup>[17]</sup> ionic liquids,<sup>[18]</sup> W/ZrO<sub>2</sub>,<sup>[19]</sup> sulfated zirconia,<sup>[20]</sup> zeolite H-BEA,<sup>[21]</sup> metal triflate,<sup>22a</sup>  $\gamma$ -Fe<sub>2</sub>O<sub>3</sub> nanoparticles,<sup>22b</sup> and sulfonic acid bonded catalysts.<sup>[23,24]</sup>

“Chitosan can coordinate metal ions (e.g. silver ions) before reduction. When metal salts were dissolved in acidified chitosan solutions, silver ions bind to the polymer chains via amino groups. Then the reduction of those ions takes place, coupled with the oxidation of the chitosan hydroxyl groups”.<sup>[25,26]</sup> The metal in nanoparticles generated the chemical bond with the electron-rich nitrogen, the one which presents in the amino groups of the polymer by using the lone electron in its valence orbital and strongly attached to the chitosan.<sup>[27]</sup> In this study, we have synthesized MnSb<sub>2</sub>O<sub>6</sub>-chitosannanocomposites and then using of MnSb<sub>2</sub>O<sub>6</sub>-chitosannanocomposites in the synthesis of coumarins via Pechmann reaction was investigated (Scheme 1).



**SCHEME 1** Synthesis of coumarins by using  $\text{MnSb}_2\text{O}_6$ -chitosan nanocomposites

## 2 | RESULT AND DISCUSSION

### 2.1 | Characterization of $\text{MnSb}_2\text{O}_6$ -chitosan nanocomposites

#### 2.1.1 | Fourier transform infrared measurements

At first,  $\text{MnSb}_2\text{O}_6$ -chitosan nanocomposites were synthesized according to the experimental section and then characterized. Figure 1 shows Fourier transform infrared (FTIR) transmission spectra of chitosan (Figure 1A), and  $\text{MnSb}_2\text{O}_6$ -chitosan nanocomposites (Figure 1B) were taken on JASCO 640 plus infrared spectrometer in the range of 4000 to 400  $\text{cm}^{-1}$  at room temperature. The FTIR spectra for chitosan are shown in Figure 1A. The broad peak observed in the region 3000 to 3700  $\text{cm}^{-1}$  has the contribution of different vibrations, namely, the hydrogen-bonded OH stretching and the  $\text{NH}_2$  asymmetric stretching. The other peaks at around 2928 and 2877  $\text{cm}^{-1}$  can be attributed to C–H symmetric and asymmetric stretching, respectively. The spectrum of chitosan showed a characteristic peak of amide at 1645  $\text{cm}^{-1}$ . The absorption bands at 1430  $\text{cm}^{-1}$  and 1174  $\text{cm}^{-1}$  assigned to O=C=O symmetric and C–O stretching vibration indicate the existence of carboxylate salt. The characteristic peak near 1112  $\text{cm}^{-1}$  is associated with the C–N vibration bond. A comparative study of the FT-IR

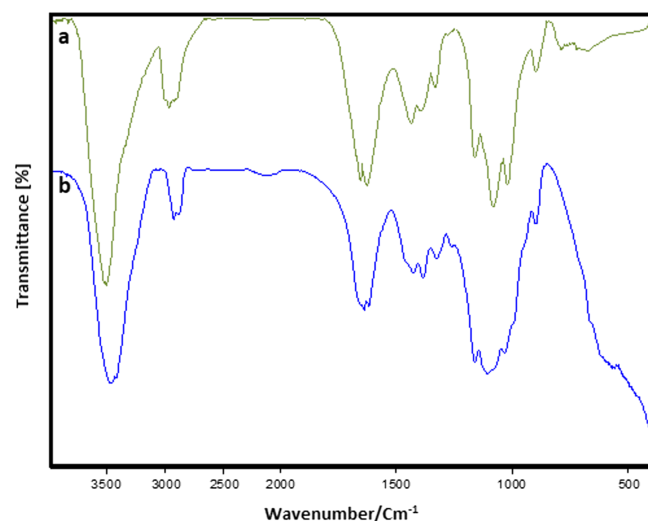


**FIGURE 1** Fourier transform infrared (FTIR) spectra of (A) chitosan and (B)  $\text{MnSb}_2\text{O}_6$ -chitosan nanocomposites [Color figure can be viewed at [wileyonlinelibrary.com](http://wileyonlinelibrary.com)]

spectrum showed that all of the peaks shifted to the lower wave number in  $\text{MnSb}_2\text{O}_6$ -chitosan nanocomposites in comparison with the chitosan (Figure 1b). The characteristic peak near 895  $\text{cm}^{-1}$ , indicating the presence of metal-C vibration bond. The above information confirmed the formation of  $\text{MnSb}_2\text{O}_6$ -chitosan nanocomposites.<sup>[28]</sup>

#### 2.1.2 | X-ray diffraction studies

Figure 2A showed X-ray powder diffraction (XRD) patterns of  $\text{MnSb}_2\text{O}_6$  nanoparticles, which revealed 12 characteristic peaks ( $2\theta = 16.58^\circ, 19.40^\circ, 22.42^\circ, 27.69^\circ, 30.32^\circ, 32.58^\circ, 35.21^\circ, 41.05^\circ, 46.50^\circ, 54.03^\circ, 61.93^\circ,$  and  $64.57^\circ$ ).<sup>[29]</sup> Figure 2B showed XRD patterns of  $\text{MnSb}_2\text{O}_6$ -chitosan nanocomposites. The nanocomposite has amorphous nature, and the strong characteristic diffraction peaks at  $2\theta = 27.69^\circ, 35.21^\circ,$  and  $54.03^\circ$  revealed that the  $\text{MnSb}_2\text{O}_6$  nanoparticles were successfully coated by

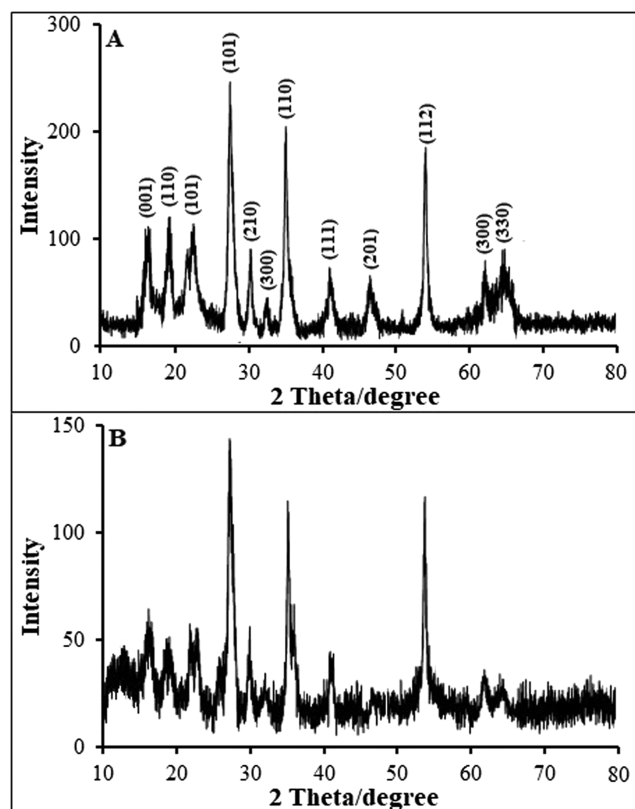


**FIGURE 2** X-ray powder diffraction (XRD) patterns of (A)  $\text{MnSb}_2\text{O}_6$  nanoparticle and (B)  $\text{MnSb}_2\text{O}_6$ -chitosan nanocomposite

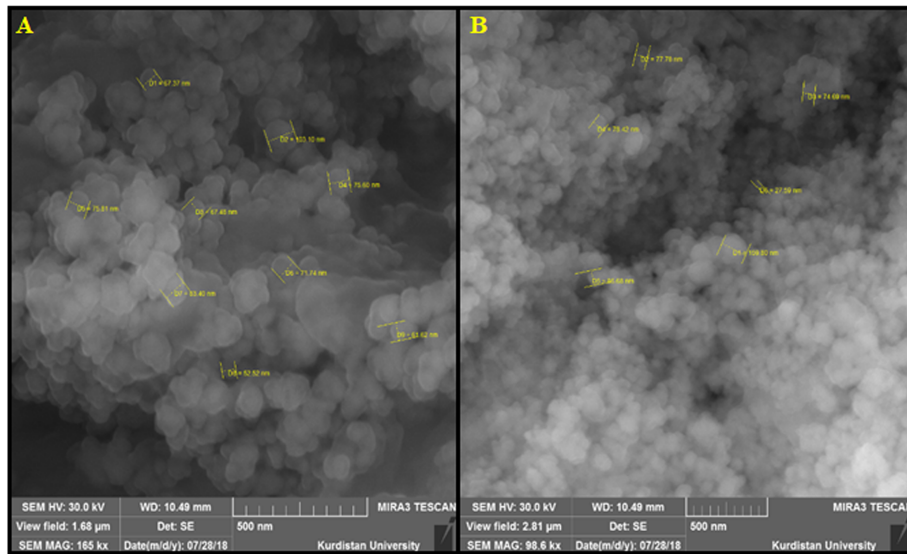


**FIGURE 3** Scanning electron microscope (SEM) images of (A)  $\text{MnSb}_2\text{O}_6$  nanoparticles and (B)  $\text{MnSb}_2\text{O}_6$ -chitosan nanocomposite [Color figure can be viewed at [wileyonlinelibrary.com](http://wileyonlinelibrary.com)]

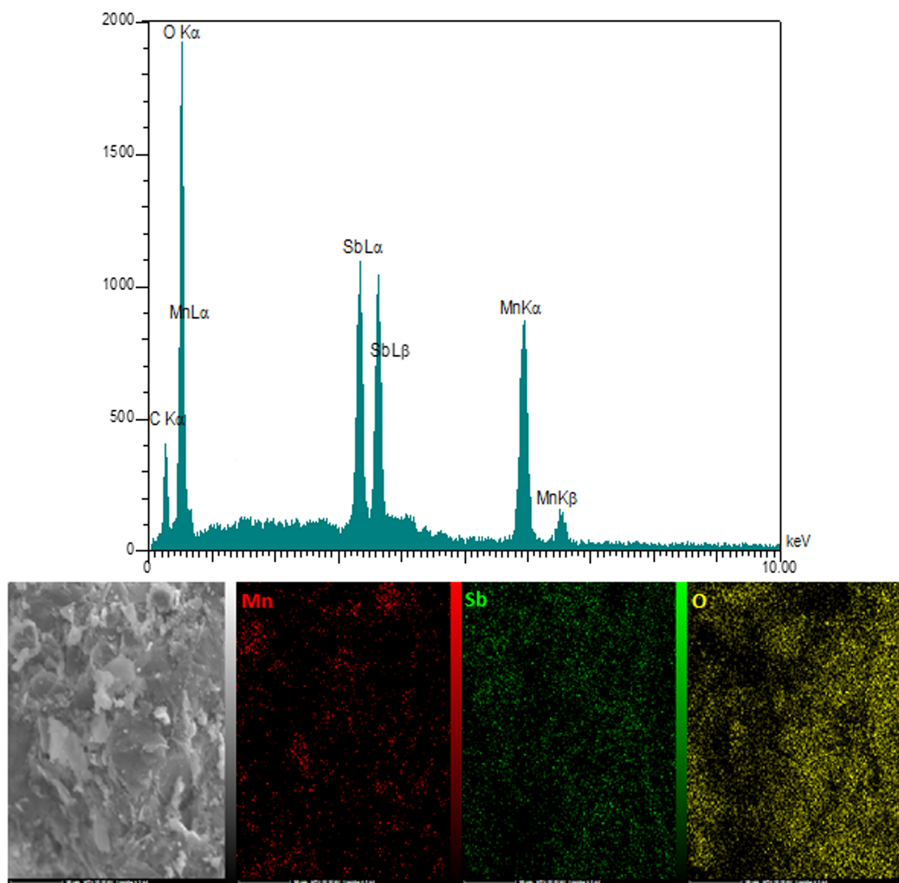


**FIGURE 4** Energy-dispersive X-ray (EDX) spectra and elemental mapping of  $\text{MnSb}_2\text{O}_6$ -chitosan nanocomposite [Color figure can be viewed at [wileyonlinelibrary.com](http://wileyonlinelibrary.com)]

amorphous chitosan “with peaks between  $2\theta$  of  $10^\circ$  and  $15^\circ$  with an amorphous structure of chitosan”.<sup>[28]</sup>

### 2.1.3 | Scanning electron microscope studies

The scanning electron microscope (SEM) images of nanoparticles of  $\text{MnSb}_2\text{O}_6$ -chitosan are shown in Figure 3. The SEM image reveals that the  $\text{MnSb}_2\text{O}_6$  nanoparticles have a spherical shape and a size ranging between 27 and 159 nm (Figure 3A). As shown in Figure 3B, the particles of  $\text{MnSb}_2\text{O}_6$ -chitosan are relatively homogeneous in shape but reveal that the nanoparticles show a large size distribution due to agglomeration. This may be due to the presence of chitosan.

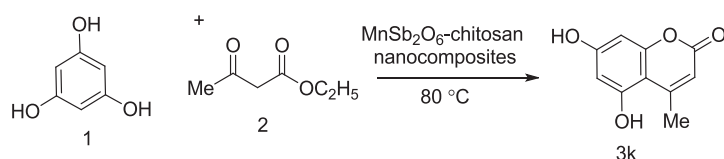
### 2.1.4 | Energy-dispersive X-ray spectroscopy

Energy-dispersive X-ray (EDX) spectroscopy was used to detect *elements* and to establish its purity as shown in Figure 4. From  $\text{MnSb}_2\text{O}_6$  nanoparticles EDX spectrum, the existence of Mn, Sb, and O is evident with no impurities. Also, it reveals the elementary distribution of different elements in particles; the EDX mapping images of Mn, Sb, and O elements are shown in Figure 4.

## 2.2 | Synthesis of coumarin derivatives

As a model catalytic reaction, ethyl acetoacetate ( $\beta$ -keto ester) and phloroglucinol (benzene-1,3,5-triol) were chosen as starting materials (Scheme 2). The effect of different solvent, different amount of catalyst, and different  $\beta$ -keto esters and phenols has been studied and presented here.

At first, we examined the influence of different solvents on this reaction such as ethanol, methanol, DMSO,  $\text{H}_2\text{O}$ , and solvent-free condition in  $80^\circ\text{C}$ , and among these, DMSO and  $\text{H}_2\text{O}$  gave the worst yield of a compound (Table 1). In fact, when we performed the reaction in DMSO and  $\text{H}_2\text{O}$ , the reaction failed (Table 1, entry 5). The best result was obtained with solvent-free condition, giving 5,7-dihydroxy-4-methyl-2H-chromene-2-one (3k) in 94% yield (Table 1, entry 5). Further screening of solvents did not improve the results (Table 1, entries 3 and 4).



**SCHEME 2** Reaction of ethyl acetoacetate and phloroglucinol

Then we carried out the optimization by varying the amount of catalyst (Table 1). Excellent yields were achieved using only 5 wt% (Table 2, entry 5). The use of a higher amount of catalyst (10-25 wt%) instead led to slight increase of yield and worse results in terms of reaction time. So, 5 wt% was chosen as the desired *catalyst amount*.

With the optimized reaction conditions in hand (5 wt% catalyst, solvent-free condition,  $80^\circ\text{C}$ ), we then examined the scope of the reaction with a variety of substrate. The results are summarized in Table 2. In general, the solvent-free reaction of phenolic derivatives with a wide range of  $\beta$ -keto ester bearing both electron-donating and electron-withdrawing substituents afforded in 88% to 99% yields.

To show the efficiency and advantage of this method, we have compared the results with the results of some of the studies reported for coumarin synthesis reaction (Table 3). Efficiency, high yields, short reaction times, simplicity of preparation of nanocomposites catalyst, and solvent-free condition are some advantages of this work.

## 2.3 | Antibacterial activity

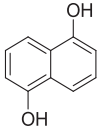
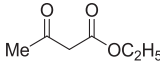
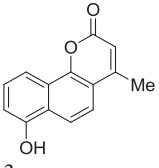
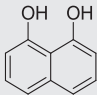
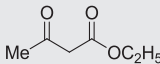
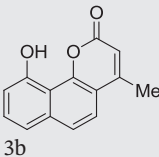
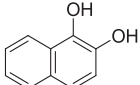
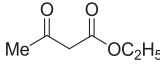
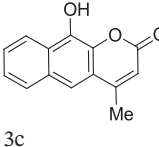
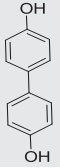
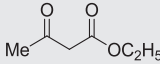
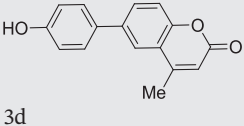
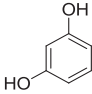
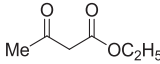
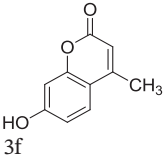
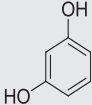
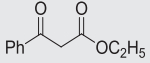
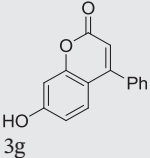
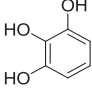
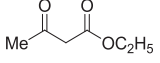
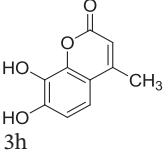
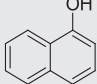
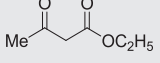
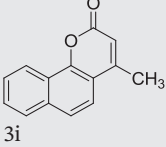
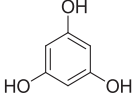
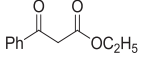
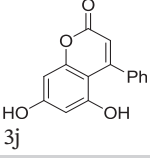
Table 4 presents the results of the antibacterial 1, 4, 7, and 10 compounds' activities. The data show that all

**TABLE 1** Optimization of the solvent and the amount of catalyst in  $80^\circ\text{C}$

Entry	Solvent	Catalyst, wt%	Time, min	Isolated Yield, %
1	EtOH	5	240	30
2	MeOH	5	240	45
3	$\text{H}_2\text{O}$	5	120	-
4	DMSO	5	1200	-
5	-	5	35	94
6	-	10	50	65
7	-	15	60	68
8	-	20	45	73
9	-	25	80	79
10	-	5 <sup>a</sup>	40	62

<sup>a</sup>Reaction condition: 5-wt%  $\text{MnSb}_2\text{O}_6$  nanoparticles in the absence of chitosan.

TABLE 2 Synthesis of coumarin derivatives

Entry	Phenol	$\beta$ -Keto Ester	Product	Time, min	Yield, %	Melting Points, °C	
						Literature Value	Reported
1			 3a	30	92	191-193°C	-
2			 3b	35	88	187-190°C	-
3			 3c	32	91	168-171°C	-
4			 3d	40	91	178-181°C	-
5			 3f	50	93	183-185°C	185-187 °C <sup>[30]</sup>
6			 3g	59	91	252-255°C	251-253 °C <sup>[30]</sup>
7			 3h	40	93	240-242°C	241-243 °C <sup>[30]</sup>
8			 3i	45	94	153-154°C	155-156 °C <sup>[31]</sup>
9			 3j	45	94	251-253°C	241-244 °C <sup>[31]</sup>

(Continues)

TABLE 2 (Continued)

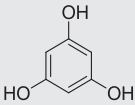
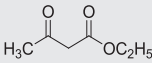
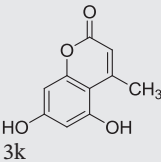
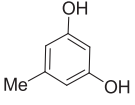
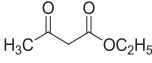
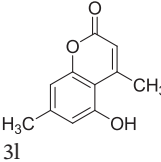
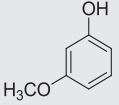
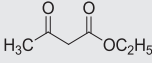
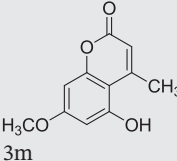
Entry	Phenol	$\beta$ -Keto Ester	Product	Time, min	Yield, %	Melting Points, °C	
						Literature Value	Reported
10				40	94	288-290°C	282-285 °C <sup>[30]</sup>
11				55	88	261-263°C	253-255 °C <sup>[30]</sup>
12				55	85	166-168°C	165-167 °C <sup>[30]</sup>

TABLE 3 Comparison of the present method with some of those reported in literatures for determination synthesis of 3k

Entry	Catalyst	Catalyst Amount	Time, min	Temperature, °C	Yield, %	Reference
1	Y (NO <sub>3</sub> ) <sub>3</sub> .6H <sub>2</sub> O	10 mol%	45	90	94	[32]
2	Zr-TMS-TFA-25	0.1 g	540	100	88	[33]
3	InCl <sub>3</sub>	10 mol%	30	65	98	[34]
4	In (OTf) <sub>3</sub>	1 mol%	32	80	87	[35]
5	Nanocrystalline sulfated tin oxide	25 wt%	240	120	95	[36]
6	ZrPW	0.2g	480	130	58	[37]
7	MnSb <sub>2</sub> O <sub>6</sub> -chitosan nanocomposites	5 wt%	40	80	94	This work

compounds exhibit favorable antibacterial characteristics towards indicator strains. Evidently, compound 3a exhibits the greatest impact towards on *Staphylococcus aureus* in comparison with other compounds.

### 3 | CONCLUSION

In conclusion, we report a simple method for the synthesis of coumarin derivatives by using MnSb<sub>2</sub>O<sub>6</sub>-chitosan nanocomposites as catalysts. The reaction proceeds in solvent-free condition and afforded high yields of the products. The synthesized compounds 3a, 3d, 3h, and 3k were evaluated for their antibacterial activity against four pathogenic bacteria (two Gram-positive and two Gram-negative). All tested compounds have shown moderate activity against *S. aureus*, and among them, compound 3a has shown the best activity.

## 4 | EXPERIMENT

### 4.1 | Materials and instrumentations

All chemicals and solvents were purchased from commercial sources and used without further purification unless otherwise stated. Melting points were determined on a Melt-Tem II melting point apparatus and are uncorrected. Infrared (IR) spectra were obtained on a Matson-1000 FTIR spectrometer. Peaks are reported in wavenumbers (cm<sup>-1</sup>). All of the NMR spectra were recorded on a Bruker model DRX-300 AVANCE (<sup>1</sup>H: 250, <sup>13</sup>C: 75 MHz) NMR spectrometer. Chemical shifts of <sup>1</sup>H and <sup>13</sup>C-NMR are reported in parts per million (ppm) from tetramethylsilane (TMS) as an internal standard in DMSO-d<sub>6</sub> as a solvent. X-ray powder diffraction (XRD) was collected on a X'Pert PRO PANalytical equipment. VEGA/TESCAN and MIRA3/TESCAN.XMU are employed to collect SEM and map images.

**TABLE 4** Antibacterial activity against Gram-positive bacteria and Gram-negative strain

Comp.	Microorganism	Inhibition Zone, mm			
		6.25 mg/mL	12.5 mg/mL	25 mg/mL	50 mg/mL
3h	<i>S aureus</i>	5±0	6±0	8±0	4±0
	<i>E coli</i>	0±0	0±0	0±0	0±0
	<i>P aeruginosa</i>	0±0	0±0	0±0	0±0
	<i>B cereus</i>	0±0	0±0	0±0	0±0
3d	<i>S aureus</i>	5±0	5±0	5±0	6±0
	<i>E coli</i>	0±0	3±0	0±0	6±0
	<i>P aeruginosa</i>	0±0	0±0	0±0	0±0
	<i>B cereus</i>	0±0	0±0	0±0	0±0
3a	<i>S aureus</i>	6±0	9±0	9±0	10±0
	<i>E coli</i>	0±0	0±0	0±0	0±0
	<i>P aeruginosa</i>	0±0	0±0	0±0	0±0
	<i>B cereus</i>	0±0	0±0	0±0	0±0
3k	<i>S aureus</i>	4±0	3±0	3±0	7±0
	<i>E coli</i>	0±0	0±0	0±0	0±0
	<i>P aeruginosa</i>	0±0	0±0	0±0	0±0
	<i>B cereus</i>	0±0	0±0	0±0	0±0

Note. The inhibition zone numbers are the average of three independent tests.

## 4.2 | Synthesis of MnSb<sub>2</sub>O<sub>6</sub>-chitosan nanocomposites

For the fabrication of MnSb<sub>2</sub>O<sub>6</sub> nanoparticles a simple solvothermal method was used by use of 1 mmol of SbCl<sub>3</sub> and 2 mmol of MnCl<sub>3</sub>·6H<sub>2</sub>O that disintegrated within 10 ml of distilled water and then NaOH solution (1.5 M) was added drop wisely to the stirring solutions until pH reached 11. The mixture of the reaction was placed into an autoclave for 4 hours at 120°C. When the autoclave temperature was cooled to room temperature (naturally), precipitates were gathered and washed using ethanol and distilled water. The resulting solid was dried (60°C, 8 hours) and then calcinated at a temperature of 700°C for a period of 5 hours. In the next step, 1 gr of MnSb<sub>2</sub>O<sub>6</sub> nanoparticles powder was poured in 1% acetic acid (100 mL), and then 1.0 gr of chitosan was added to the solution and sonicated for 30 minutes. Then the NaOH solution (0.10M) was added dropwise until pH reached 7 under stirring. The mixture was kept under stirring at 75°C to 80°C for 3 hours. Finally, the reaction mixture was filtrated and washed with distilled water many times and dried at 50°C to obtain MnSb<sub>2</sub>O<sub>6</sub>-chitosan nanocomposites.

## 4.3 | General procedure for the synthesis of coumarin derivatives (3a-m)

A mixture of a phenolic substrate (1 mmol) and β-keto ester (1 mmol) and MnSb<sub>2</sub>O<sub>6</sub>-chitosan nanocomposites (5 wt%) was stirred in an oil bath (80°C). After

completion of the reaction at the desired time as indicated in Table 2, the solid product was poured onto water (20 mL). The solid product obtained was filtered off and recrystallized from hot ethanol to obtain the pure product.

## 4.4 | Spectra data

### 4.4.1 | 3a: 7-Hydroxy-4-methyl-2H-benzo[h]chromen-2-one

mp 191-193°C; Yield 92%. IR (KBr, cm<sup>-1</sup>): 3350 (OH), 1660 (C=O). <sup>1</sup>H-NMR (250 MHz, DMSO): δ = 8.41 (s, 1H, OH), 8.40-8.39 (m, 1H), 7.72 (d, 1H, J = 7.0 Hz, H-Ar), 7.53 (d, 1H, J = 7.5 Hz, H-Ar), 7.39 (t, 1H, J = 4.5 Hz, H-Ar), 6.18 (d, 1H, J = 8 Hz, H-Ar), 6.17 (s, 1H), 2.36 (s, 3H, CH<sub>3</sub>). <sup>13</sup>C-NMR (75 MHz, DMSO): δ = 161.2, 154.7, 152.6, 128.3, 127.9, 122.8, 120.8, 117.0, 112.9, 112.3, 110.2, 19.2, 18.58.

### 4.4.2 | 3b: 10-Hydroxy-4-methyl-2H-benzo[h]chromen-2-one

mp 187-190°C; Yield 88%. IR (KBr, cm<sup>-1</sup>): 3423 (OH), 1706 (C=O). <sup>1</sup>H-NMR (250 MHz, DMSO): δ = 9.04 (s, 1H)OH, 7.8 (d, 1H, J = 7.25 Hz, H-Ar), 7.73 (d, 1H, J = 7.25 Hz, H-Ar), 7.43 (t, 1H, J = 6 Hz, H-Ar), 7.22 (d, 1H, J = 7.5 Hz, H-Ar), 6.28 (d, 1H, J = 7 Hz, H-Ar), 6.25 (s, 1H, H-Ar), 2.43 (s, 3H, CH<sub>3</sub>). <sup>13</sup>C-NMR (75 MHz, DMSO): δ = 160.2, 154.7, 153.1, 152.9, 133.7,

125.9, 124.7, 120.5, 120.1, 113.6, 11.9, 110.9, 109.7, 18.9, 18.58.

#### 4.4.3 | 3c: 10-Hydroxy-4-methyl-2H-benzo [g]chromen-2-one

mp 168–171°C; Yield 91%. IR (KBr,  $\text{cm}^{-1}$ ): 3416 (OH), 1699 (C=O).  $^1\text{H-NMR}$  (250 MHz, DMSO):  $\delta$  = 9.88, OH, (s, 1H), 8.15 (d, 1H,  $J=7.5\text{Hz}$ , H-Ar), 7.72 (d, 1H,  $J = 7.5\text{Hz}$ , H-Ar), 8.04 (d, 1H,  $J = 7.75\text{Hz}$ , H-Ar), 7.7 (t, 1H,  $J = 6.25\text{Hz}$ , H-Ar), 7.5 (t, 1H,  $J = 6\text{Hz}$ , H-Ar), 7.11 (s, 1H, H-Ar), 6.26 (s, 1H, H-Ar), 2.47 (s, 3H,  $\text{CH}_3$ ).  $^{13}\text{C-NMR}$  (75 MHz, DMSO):  $\delta$  = 163.1, 161.7, 153.2, 133.2, 132.6, 128.9, 127.5, 126.1, 125.8, 123.7, 121.3, 120.9, 111.9, 19.9.

#### 4.4.4 | 3d: 6-(4-Hydroxyphenyl)-4-methyl-2H-chromen-2-one

mp 178–181°C; Yield 91%. IR (KBr,  $\text{cm}^{-1}$ ): 3449 (OH), 1729 (C=O).  $^1\text{H-NMR}$  (250 MHz, DMSO):  $\delta$  = 9.67 (s, 1H), OH, 7.97 (s, 1H, H-Ar), 7.79 (d, 1H,  $J = 7.5\text{Hz}$ , H-Ar), 7.55 (d, 1H,  $J = 5\text{Hz}$ , H-Ar), 7.41–7.42 (m, 2H, H-Ar), 6.83–6.84 (m, 2H, H-Ar), 6.27 (s, 1H, H-Ar), 2.43 (s, 3H),  $\text{CH}_3$ .  $^{13}\text{C-NMR}$  (75 MHz, DMSO):  $\delta$  = 160.0, 156.3, 152.7, 151.8, 137.9, 132.1, 129.8, 127.9, 126.8, 121.2, 120.4, 115.8, 113.1, 20.1.

### 4.5 | Determination of antibacterial activity

The 3a, 3d, 3h, and 3k compounds' antibacterial behavior towards four pathogenic bacteria (Gram-positive bacteria: *S aureus* and *Bacillus cereus* and two Gram-negative: *Escherichia coli* and *Pseudomonas aeruginosa*) were evaluated using the disc diffusion technique with 100  $\mu\text{L}$  of suspension possessing  $10^6$  CFU/mL bacteria, dispersed on Muller-Hinton agar (MHA) medium. Sterile paper discs of 6 mm diameter were then saturated using various compound concentrations (6.25, 12.5, 25, and 50 mg/mL) and put onto a Muller-Hinton agar. These plates were placed into incubation for 18 to 24 hours at a temperature of 37°C. Upon the completion of this period, the clear zone diameter at the disk vicinity was measured and presented in terms of millimeters as relevant antibacterial behavior. Every test was run three times, and the resulting data were expressed as mean  $\pm$  standard deviation (SD).

### ORCID

Dadkhoda Ghazanfari  <https://orcid.org/0000-0003-0148-2462>

Enayatollah Sheikhsosseini  <https://orcid.org/0000-0003-2973-9768>

### REFERENCES

- [1] M. C. O. Villamizar, C. E. P. Galvis, L. Y. V. Méndez, V. V. Kouznetsov, Coumarin-Based Molecules as Suitable Models for Developing New Neuroprotective Agents Through Structural Modification, in *Discovery and Development of Neuroprotective Agents from Natural Products*, Elsevier, Amsterdam **2018** 149.
- [2] R. O'Kennedy, R. D. Thornes, *Coumarins: Biology, Applications and Mode of Action*, Wiley and Sons, Chichester **1997**.
- [3] L. A. Singer, N. P. Long, *J. Am. Chem. Soc.* **1966**, *86*, 5213.
- [4] M. Zahradnik, *The Production and Application of Fluorescent Brightening Agents*, Wiley, New York **1992**.
- [5] C. Wu, J. Wang, J. Shen, C. Bi, H. Zhou, *Sensor Actuat B-Chem* **2017**, *243*, 678.
- [6] H. Von Pechmann, C. Duisberg, *Chem. Ber.* **1884**, *17*, 929.
- [7] J. R. Johnson, *Org. React.* **1942**, *1*, 210.
- [8] (a) G. Jones, *Org. React.* **1967**, *15*, 204. (b) G. Brufola, F. Fringuelli, O. Piermatti, H. Pizzo, *Heterocycles*. **1996**, *43*, 1257.
- [9] R. L. Shirner, *Org. React.* **1942**, *1*, 1.
- [10] I. Yavari, R. Hekmat-Shoar, A. Zonouzi, *Tetrahedron Lett.* **1998**, *39*, 2391.
- [11] A. Ramani, B. M. Chanda, S. Velu, S. Sivansaker, *Green Chem.* **1999**, *1*, 163.
- [12] F. Bigi, L. Chesini, R. Maggi, G. Sartori, *J. Org. Chem.* **1999**, *64*, 1033.
- [13] M. C. Laufer, H. Hausmann, W. F. Holderich, *J. Catal.* **2003**, *218*, 315.
- [14] D. A. Chaudhari, *Chem. Ind.* **1983**, *568*, 14.
- [15] R. Hinze, M. C. Laufer, W. F. Holderich, W. Bonrath, T. Netscher, *Catal. Today* **2009**, *140*, 105.
- [16] E. A. Gunnewegh, A. J. Hoefnagel, H. van Bekkum, *J. Mol. Catal. A: Chem.* **1995**, *100*, 87.
- [17] S. Frere, V. Thiery, T. Besson, *Tetrahedron Lett.* **2001**, *15*, 2791.
- [18] Y. Gu, J. Zhang, Z. Duan, Y. Deng, *Adv. Synth. Catal.* **2005**, *347*, 512.
- [19] B. M. Reddy, V. R. Reddy, D. Giridar, *Synth. Commun.* **2001**, *31*, 3603.
- [20] B. Tyagi, M. K. Mishra, R. V. Jasra, *J. Mol. Catal. A: Chem.* **2008**, *286*, 41.
- [21] A. J. Hoefnagel, E. A. Gunnewegh, R. S. Downing, H. van Bekkum, *J. Chem. Soc. Chem. Commun.* **1995**, 225.
- [22] a) L. Wang, J. Xia, H. Tian, C. Qian, Y. Ma, *Indian J. Chem.* **2003**, *42B*, 2097. b) Z. Abbasi, S. Rezayati, M. Bagheri, R. Hajinasiri, *Chin. Chem. Lett.* **2017**, *28*, 75.
- [23] K. Niknam, D. Saberi, M. Baghernejad, *Chin. Chem. Lett.* **2009**, *20*, 1444.
- [24] B. Karimi, D. Zareyee, *Org. Lett.* **2008**, *10*, 3989.



- [25] H. V. Tran, L. Dai Tran, C. T. Ba, H. D. Vu, T. N. Nguyen, D. G. Pham, P. X. Nguyen, *Colloids Surf.* **2010**, *360*, 32.
- [26] D. W. Qian, *Colloids Surf.* **2008**, *62*, 136.
- [27] A. H. Pakiari, Z. Jamshidi, *J. Phys. Chem.* **2007**, *111*, 4391.
- [28] A. A. Saad, A. M. Azzam, S. T. El-Wakeel, B. B. Mostafa, M. B. Abd El-latif, *Environ.l Nanotechnol. Monit. Manag.* **2018**, *9*, 67.
- [29] V. B. Nalbandyan, E. A. Zvereva, A. Y. Nikulin, I. L. Shukaev, M. H. Whangbo, H. J. Koo, M. Abdel-Hafiez, X. J. Chen, C. Koo, A. N. Vasiliev, R. Klingeler, *Inorg. Chem.* **2015**, *54*, 1705.
- [30] B. Karami, M. Kiani, *Cat. Com.* **2011**, *14*, 62.
- [31] V. Kumar, S. Tomar, R. Patel, A. Yousaf, V. S. Parmar, S. V. Malhotra, *Synth. Commun.* **2008**, *38*, 2646.
- [32] K. Jung, Y. J. Park, J. S. Ryu, *Synth. Commun.* **2008**, *38*, 4395.
- [33] P. Kalita, R. Kumar, *Microporous Mesoporous Mater.* **2012**, *149*, 1.
- [34] B. Karami, S. Khodabakhshi, M. Jamshidi, *J. Chin. Chem. Soc.* **2013**, *60*, 1103.
- [35] B. Karami, M. Kiani, M. A. Hoseini, *Chinese. J. Catal.* **2014**, *35*, 1206.
- [36] A. I. Ahmed, S. A. El-Hakam, A. S. Khder, W. A. El-Yazeed, *J. Mol. Catal. A-Chem* **2013**, *366*, 99.
- [37] S. Ghodke, U. Chudasama, *Appl Catal A* **2013**, *453*, 219.

## SUPPORTING INFORMATION

Additional supporting information may be found online in the Supporting Information section at the end of the article.

**How to cite this article:** Bahramnezhad B, Ghazanfari D, Sheikhsosseini E, Akhgar MR, Ahmadi SA. MnSb<sub>2</sub>O<sub>6</sub>-chitosan nanocomposite: An efficient catalyst for the synthesis of coumarins via Pechmann reaction. *J Heterocyclic Chem.* 2019;1–9. <https://doi.org/10.1002/jhet.3763>